Journal of Materials Processing Technology 240 (2017) 168–175

Contents lists available at ScienceDirect

Journal of Materials Processing Technology

journal homepage: www.elsevier.com/locate/jmatprotec

40 kJ magnetic pulse welding system for expansion welding of aluminium 6061 tube

Shobhna Mishra[a,*], Surender Kumar Sharma[a], Satendra Kumar[b], Karuna Sagar[a], Manraj Meena[a], Anurag Shyam[a]

[a] Energetic & Electromagnetic Division, Bhabha Atomic Research Centre, Visakhapatnam, India
[b] Accelerator& Pulsed PowerDivision, Bhabha Atomic Research Centre, Mumbai, India

ARTICLE INFO

Article history:
Received 2 June 2016
Received in revised form 25 August 2016
Accepted 23 September 2016
Available online 28 September 2016

Keywords:
Magnetic pulse welding
Magnetic field diffusion
Impact velocity

ABSTRACT

The use of aluminium alloys has increased significantly in industries, so this trend has spurred the development of new joining methods for aluminium alloys. A 40 kJ Magnetic Pulse Welding (MPW) system was designed and developed to carry out the Electro-Magnetic (EM) expansion welding of aluminium 6061 alloy tube. The system consists of 15 kV, 356 μF capacitor bank, spark-gap switch and an EM expansion welding coil. The short circuit frequency of the MPW system is 20 kHz; it had delivered the maximum current of 166 kA, magnetic field of 31 T in the 1.5 μH coil and has achieved the maximum impact velocity of 660 m/s for 65 mm diameter, 1.5 mm thick tube. The EM expansion coils were designed and fabricated using circular and rectangular cross section copper wires. For the same discharge current, coils fabricated with rectangular cross section copper wires were found mechanically stronger and developed about 1.3 times higher fields than the coils fabricated of circular cross section copper wires. Simulation and experimental studies have been done to analyse the effect of factors like system frequency, peak current, magnetic field profile and geometry of work piece on the quality of weld obtained in the process. Expansion welding of Al 6061 tube of 25 mm to 65 mm diameter, 1.5 mm and 2 mm thickness and stand-off distance 2 mm to 3 mm was carried out. A stand-off distance of 2.5 mm was found to be the optimal value for a 65 mm diameter, 1.5 mm tube at a discharge current of 166 kA, which resulted into a good and strong metallurgical bond between the work pieces at the interface. Thicker tubes require comparatively more energy to deform significantly and to get accelerated to required velocity in comparison to thinner tubes. The characterization of the weld joint was done by drop, pull out, peel-off tests and microscopic image of the weld joint was also analysed to confirm the wavy morphology of the weld interface.

1. Introduction

Magnetic Pulse Welding (MPW) technique is a high speed solid state joining process and has been applied for production of drive shafts and vehicle frames in the automotive industry as stated by Miranda et al. (2014), Umer (2013). Rajawat et al. (2004) have claimed that the MPW technique has variety of applications in the industry and is also currently catering to the development as a nuclear reactor technology. It is a non-contact technique where in the discharged damped current induces a strong transient magnetic field in the coil. The work piece placed over the coil cuts the transient magnetic field and eddy current starts flowing through the work piece which generates a magnetic pressure causing one work piece to hit the other work piece with greater impacts. This magnetic pressure generated accelerates the work piece towards each other and subsequently joining the two materials. Lee and Lee (1996) reported that the magnetic pressure developed during the process depends on the geometry and resistivity of the workpiece. Miranda et al. (2014) claimed that aluminium alloys, being light in weight, are best suitable for application in aerospace, nuclear, shipbuilding, railway, appliances and automobile industries. They also stated that for improved fuel economy and reduced CO_2 vehicle emission for environmental benefits, low-cost and light-weight materials are gaining demand in major automobile industries. Aluminium 6061 finds its wide application in aircraft and aerospace industries, in marine fittings, in camera lenses, electrical fittings, automotive parts and alike. Jassim (2011) indicated that aluminium possesses high thermal conductivity, high thermal expansion coefficient, low melting temperature making it's welding different than others. He also highlighted the advantage of MPW technique over

* Corresponding author.
E-mail address: shobhnamishra89@gmail.com (S. Mishra).

http://dx.doi.org/10.1016/j.jmatprotec.2016.09.020
0924-0136/

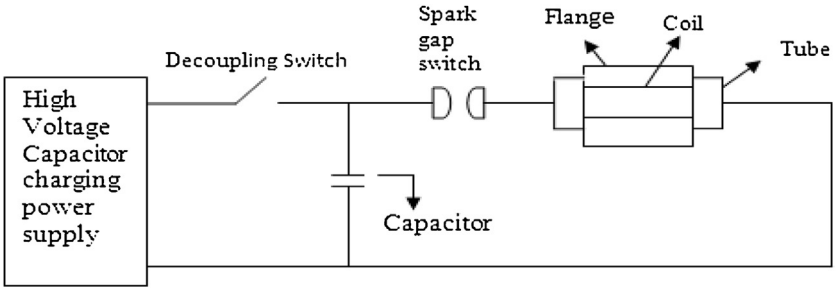

Fig. 1. Schematic of Magnetic Pulse Welding circuit.

traditional welding techniques is that a tubular weld joint can be produced in less than a second and in welding aluminium, it does not produce the heat-affected zone and/or other weld defects, which are typical of conventional fusion welding processes. Moreover, for heat treated aluminium alloys, joints of very good quality can be produced with this technique. This welding technique is presently used in limited application such as sheet to sheet and compression welding of tubes, but the expansion welding of tube to flange is not studied and reported yet. Loncke (2009); Broeckhove and Willemsens (2009–2010) have reported about the magnetic pulse welding of aluminium sheet to aluminium sheet and compressive welding of aluminium tube to aluminium tube but the expansion welding of aluminium tube to aluminium flange has not been much explored yet.

The basics of the MPW process consist of three principle parts: a capacitor bank to store and release energy, coil to create the magnetic field, and work piece to be formed or welded. Broeckhove and Willemsens (2009–2010); Loncke (2009); Desai et al. (2010b) and Umer (2013) claimed that in order to achieve a good weld joint, the technique demands that the job pieces should have high impact velocity at the time of collision. Due to this high impact velocity a jet is created along the surface of the weld and a substantial amount of the work piece material is moved by this jet force eliminating the need of pre-cleaning processes. Zhidan et al. (2013); Kore et al. (2012); Patel et al., (2009) and Loncke (2009) reported that a wavy morphology bond interface is formed with occasional laminar interface morphology and this transition zone might be caused by mechanical mixing, intensive plastic deformation and/or melting, resulting into a metallurgical bond between the work pieces at the interface. In deciding this collision velocity, material of the work piece, geometrical parameters and electrical properties are seen to play a crucial role, as stated by Al Hassani et al. (1967). Umer (2013) and Desai et al. (2010a) reported that it was explicitly established that the collision velocity required to achieve weld was more than 400 m/s which is independent of job size and material. Loncke (2009) claimed that impact velocity range found for aluminium was 400 m/s–1000 m/s. In this technique, the impact or collision velocity is generated by the discharge current of a capacitor bank. Though the technique has been used with some success in the automotive industry and in research laboratories, it has failed to enter the general manufacturing industry.

2. Magnetic pulse welding system

A 20 kJ MPW system consisting of 178 μF/15 kV/20 kJ capacitor bank was initially designed and commissioned, which was then expanded to 40 kJ capacity with 356 μF/15 kV/40 kJ capacitor bank. The system consists of a capacitor bank, spark-gap switch, high voltage power supply, trigger generator, coil and the work pieces. The schematic diagram of the expansion welding system is shown in Fig. 1.

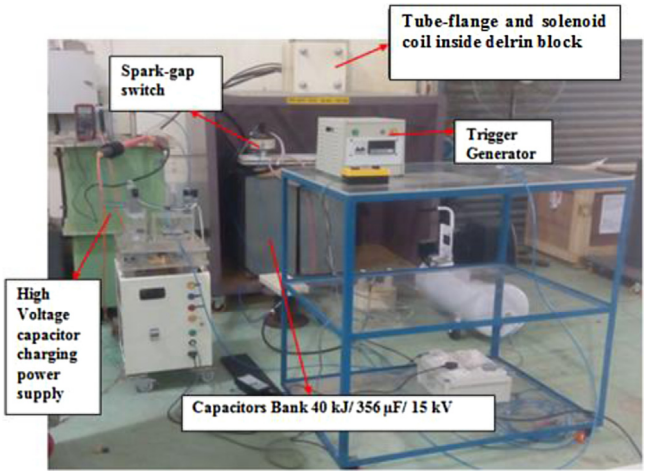

Fig. 2. Experimental setup.

The MPW system has a 356 μF/15 kV/40 kJ capacitor bank, the trigger spark-gap switch is mounted on the top of the capacitor, which can be pressurized by air up to 4 atm for operating at higher voltages and higher energy levels, as shown in Fig. 2. Four numbers of URM-67 cables of 1 m each were used to connect the spark-gap switch to the coil. The total inductance of the system was less than 200 nH and the short circuit discharge frequency of the system is 20 kHz. The capacitor bank is charged using a 15 kV/100 mA high voltage power supply. The capacitor bank and its power supply were isolated using a pneumatically operated decoupling switch after charging it to the rated voltage. The spark-gap switch is triggered by electrical pulse, resulting in discharge of capacitor bank energy to the coil. The discharging circuit consists of a spark gap switch, the coil and the aluminium tube-flange work pieces. The capacitor bank voltage is monitored with resistive voltage divider of 1000:1 attenuation and the discharge current is measured with integrated rogowski coil of 1 V/100 kA sensitivity.

3. MPW coil design for expansion welding

For expansion welding of Al 6061tube-flange work piece, a solenoid coil was designed and fabricated taking the work piece geometrical dimensions into considerations. To design the coil, the collision velocity was chosen to be 500 m/s, so as to achieve good weld. Vinitha et al. (2014) reported that due to the impact caused by the tube on the flange, severe plastic deformation occurs at the tube-flange interface causing a metallurgical bond between the two work pieces.The capacitor discharge current induces current in the inner tube, this induced current tends to penetrate the tube thickness. The depth of penetration known as skin depth depends

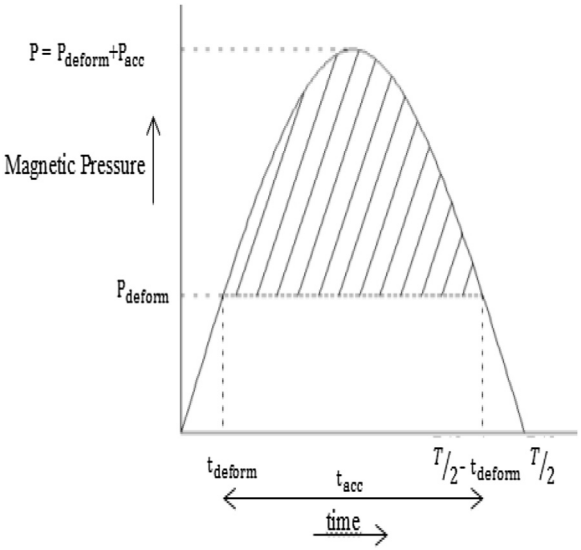

Fig. 3. The pressure pulse on a tubular work piece with a coil (Loncke, 2009).

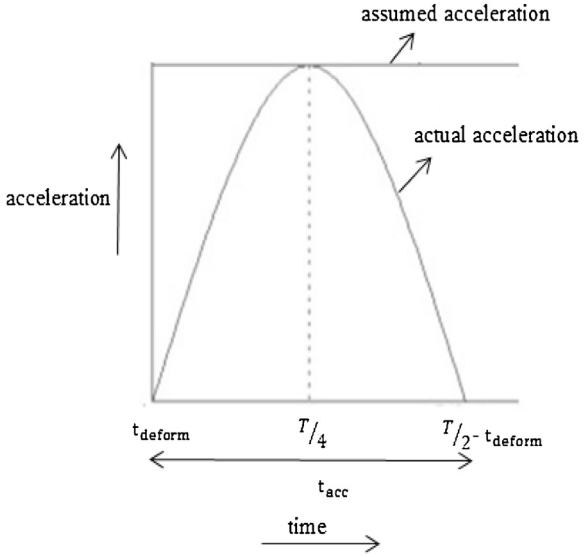

Fig. 4. Assumed and actual acceleration pulse that will occur due to the magnetic pressure (Loncke, 2009).

upon the material electrical conductivity, magnetic permeability and system frequency, as given by (1):

$$\delta = 1/\sqrt{\pi\sigma\mu f} \tag{1}$$

Where δ is the skin depth, f is the frequency of the discharge current, μ the magnetic permeability of the work piece and σ is the electrical conductivity of the work piece. A system frequency above 6 kHz, as calculated, is necessary to limit the diffusion of magnetic field within tube thickness of 1.5 mm. The magnetic pressure, P, is the summation of pressure required to deform, P_{defrom}, and the pressure, P_{acc} to accelerate the tube work piece. Vinitha et al. (2014), Loncke (2009), Broeckhove and Willemsens (009–2010) stated that the magnetic pressure can be obtained using (2, 3) for a tube of radius (R), thickness (t), and stand-off distance (s). The magnetic pressure initially rises, and then falls after reaching the peak pressure, as seen in Fig. 3.

$$P = P_{defrom} + P_{acc} \tag{2}$$

$$P = t[\rho V_c^2/2.s + 2\sigma_y/R] \tag{3}$$

Where ρ is the density of the tube material (kg/m^3), V_c is the impact velocity (m/s), and σ_y is the yield strength of the tube (MPa).

Loncke (2009) reported that it was assumed that the velocity increases up to the required velocity, V_c until impact due to a constant acceleration during the whole movement. The acceleration is in reality not constant but pulse acceleration, as seen in Fig. 4. This is because the pressure applied on the tube is a pulse and not a constant load as it is directly related to the value of the magnetic pulse. The work piece deforms in time t_{deform}, as seen in Fig. 3 and by this time the pressure reaches a value equal to the pressure required for tube deformation, P_{deform}. The tube then starts accelerating and the required maximum acceleration is associated with the maximum

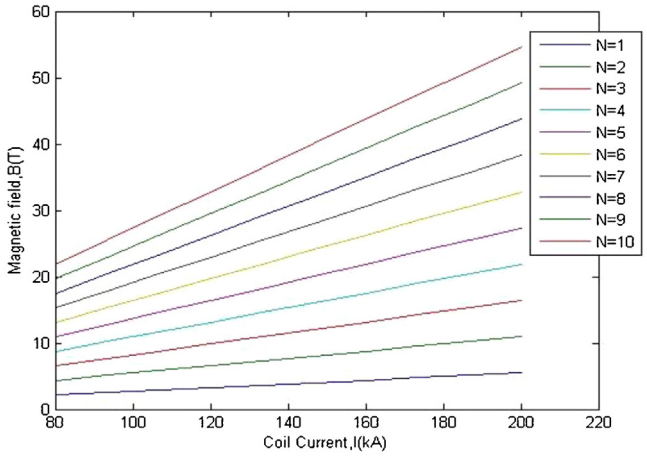

Fig. 5. Variation of magnetic field developed with current discharged into the coil.

value of the magnetic pressure, P and where t_{acc} is the total time of acceleration and deacceleration, as seen in Fig. 4.For a frequency, f, the maximum pressure, P and the acceleration is reached at time $T/4$, where $T = 1/f$.

Loncke (2009), Broeckhove and Willemsens (2009–2010) also stated that the magnetic field, B, required can be calculated using (4)

$$P = (B^2/2\mu) \times \left(1 - exp^{-2t/\delta}\right) \tag{4}$$

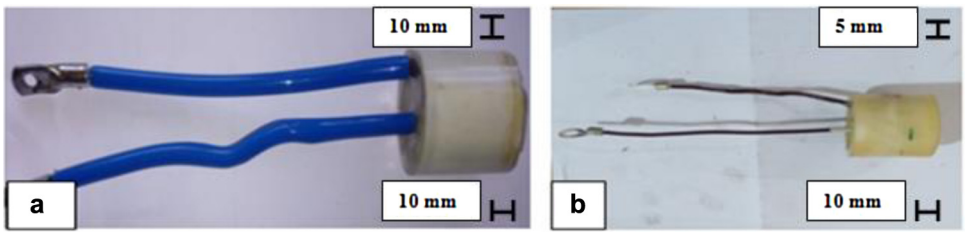

Fig. 6. Designed and fabricated solenoid coil (a) rectangular cross-section copper coil (b) circular cross-section copper coil.

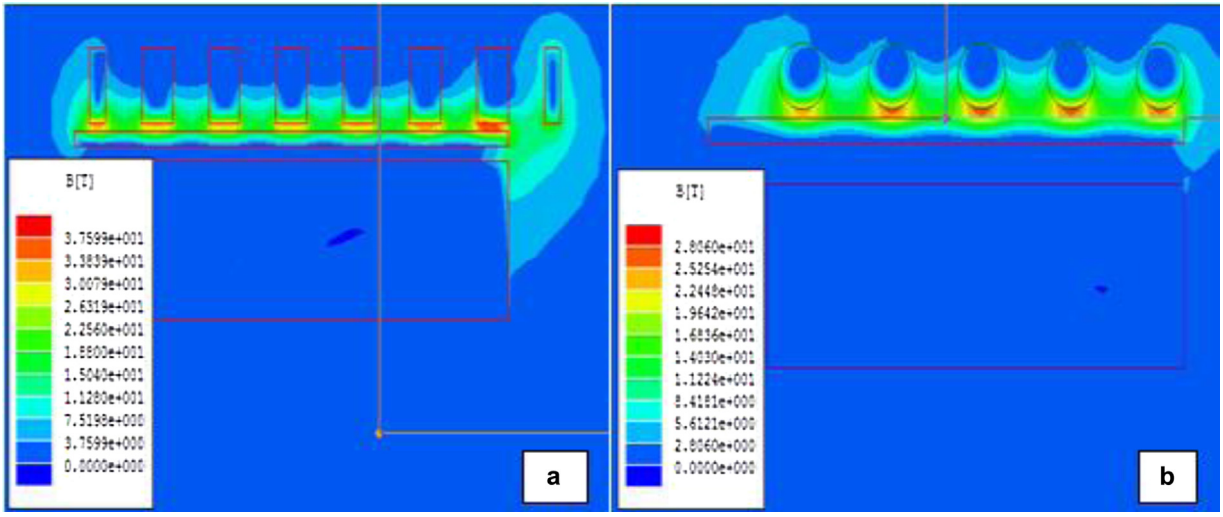

Fig. 7. Magnetic field developed for I = 120 kA, frequency, f = 6 kHz (a) with rectangular cross-section coil is 37 T and (b) with circular cross-section coil for current is 28 T, from MAXWELL SV simulation studies.

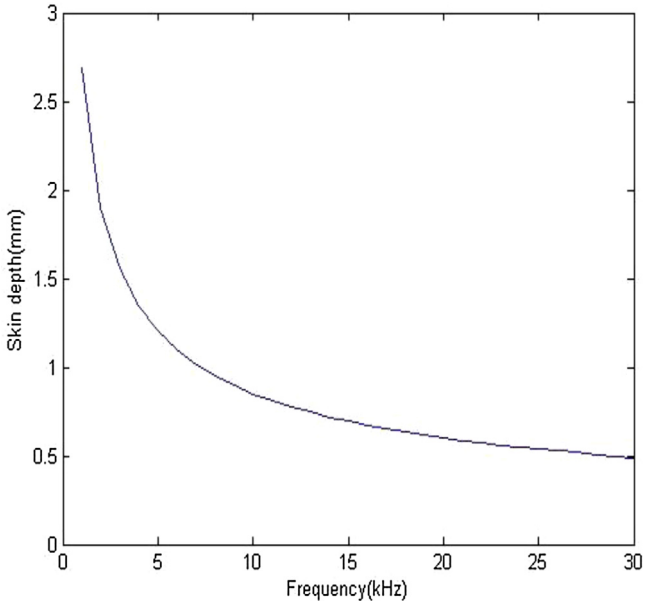

Fig. 8. Variation of skin depth with frequency.

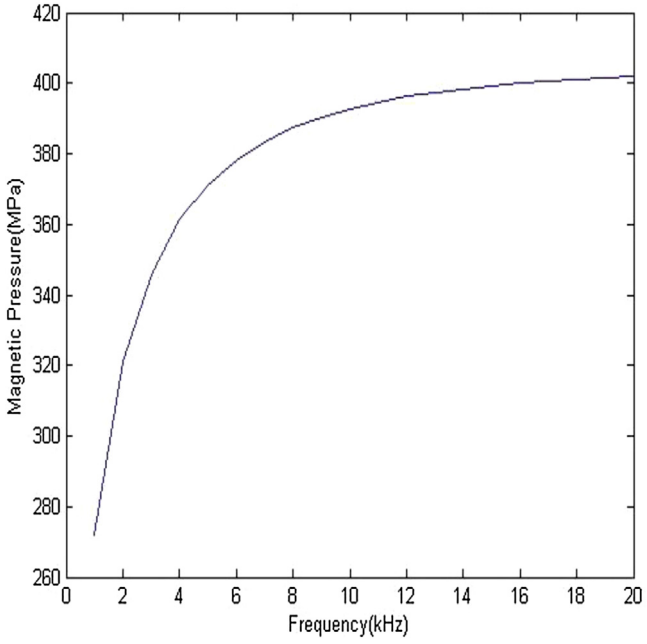

Fig. 9. Variation of Magnetic pressure with frequency.

Moreover, the peak current, *I*, corresponding to a magnetic field value depends upon the number of turns, *N*, in the solenoid coil and can be calculated using (5)

$$B = (\mu NI)/l \tag{5}$$

The number of turns in the coil is decided based upon the copper wire cross-section that makes the solenoid coil conductor, the allowed length of the solenoid coil, *l* and the inter-turn gap permitted to prevent dielectric failure. MATLAB code simulation was done for discharge current between 80 kA to 200 kA. Lower limit 80 kA, as shown in Fig. 5 corresponds to 15 T magnetic field necessary to generate the required pressure to deform and accelerate the tube. The upper bound of 200 kA is the maximum current that can be discharged from the designed 40 kJ system. It was observed that for a particular number of turns, *N*, of the solenoid coil, the developed magnetic field increases with the increase in discharge coil current, as shown in Fig. 5.

The number of turns of solenoid coil, *N*, was set to 7, for which the peak current was about 166 kA for a magnetic field value of around 31 T over a solenoid coil length of 45 mm. The total system inductance, *L*, was calculated using (6), of which the coil inductance was determined using (7) and was also measured with an inductance-meter.

$$f = 1/2\pi\sqrt{LC} \tag{6}$$

$$L_c = \left(\mu N^2 A\right)/l \tag{7}$$

Where *l* is length of solenoid coil, *A* is the area of solenoid coil conductor, as $A = \pi r^2$ and r is the radius of the solenoid coil conductor. The charging voltage was calculated, using (8), where *k* is the reversal factor and total inductance, *L*, is calculated using (6).

$$V = \left(I/k\right)/\sqrt{\frac{C}{L}} \tag{8}$$

Based on the calculations, fabrication of single layer epoxy reinforced solenoid coil for 25 mm, 50 mm and 65 mm diameter tube

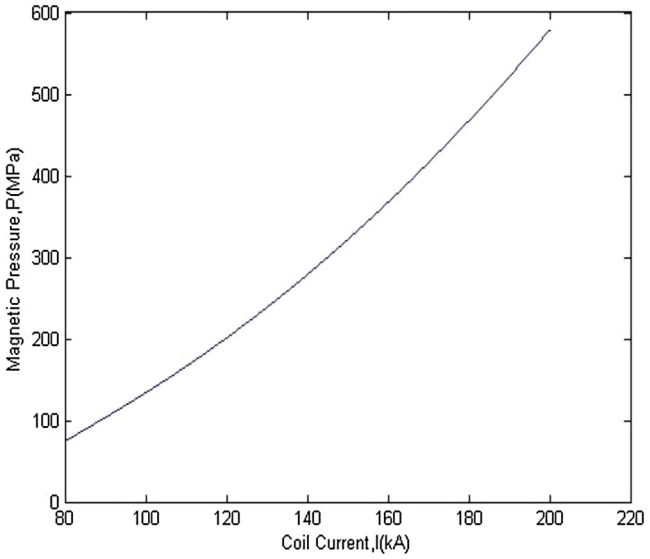

Fig. 10. Variation of magnetic pressure with coil current.

was done using rectangular cross-section copper wires, as seen in Fig. 6a and circular cross-section copper wires, as seen in Fig. 6b.

Fabrication and epoxy-reinforcement of expansion solenoid coils for smaller diameter i.e. 25 mm tube was difficult. Moreover, diffusion time constant, τ as in Eq. (9), which signifies the duration that the magnetic field takes to diffuse through the work piece should be much higher than the response time i.e. $T/4$ of the system as seen in Figs. 3 and 4. It was also stated by Koreaki and Matatoshi (1988) that larger the outer diameter to thickness ratio of the tube, the more feasible the welding becomes.

$$\text{Diffusion time constant, } \tau = \frac{\sigma \mu R t}{2}. \quad (9)$$

Where R is the radius of tube, t is the thickness of the tube, σ is the electrical conductivity and μ is the magnetic permeability.

Hence, simulation and experiments were mostly concentrated on 50 mm and 65 mm coil and tube-flange pair. From Ansoft MAXWELL SV 2D simulation studies as seen in Fig. 7, for the same area of cross-section, same pitch maintained between the turns and for the same discharge current, about 1.3 times higher magnetic fields were developed with coils fabricated from rectangular cross-section copper wires. Moreover, based on experimental results coils fabricated with rectangular cross-section copper coils were found mechanically stronger than the coils fabricated with circular cross-section copper coils.

Fig. 12. Diametrical expansion of 65 mm diameter tube of 1.5 mm and 2 mm thick, at voltage 9 kV and current 120 kA.

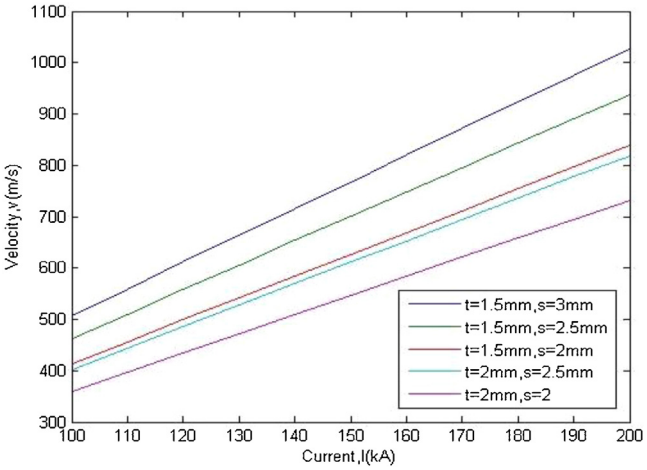

Fig. 13. Variation of impact velocity with coil current for various combinations of tube thickness and stand-off distance.

4. Expansion welding of Al 6061

MPW was performed on Al 6061 tube to Al 6061 flange by varying the geometrical parameters like the thickness of tube, diameter of tube, stand-off distance and energy level. MATLAB code simulation studies were done with tube thickness of 1.5 mm and 2 mm, stand-off distance of 2 mm, 2.5 mm and 3 mm,and varying tube radius from 12 mm to 50 mm. Experiments were concentrated on tube radius in the range of 15 mm to 33 mm,with tube thickness and stand-off distance same as in simulation. Experiments were done at different energy levels with two variants of solenoid conductors i.e. coils fabricated with circular cross-section and rectangular cross-section copper wires. To ensure safety, concentricity and that the pressures generated are effectively utilized in causing a good impact between the two work pieces, the solenoid coil conductor

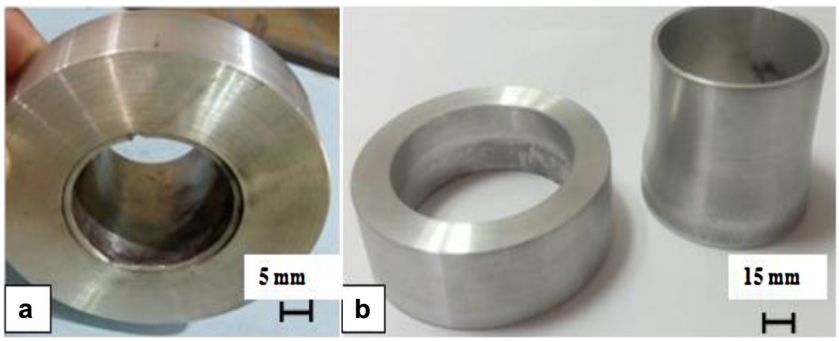

Fig. 11. (a) 25 mm diameter welded tube-flange that passed the drop, pull and peel off tests. (b) 50 mm diameter tube-flange that failed in the drop and pull out tests.

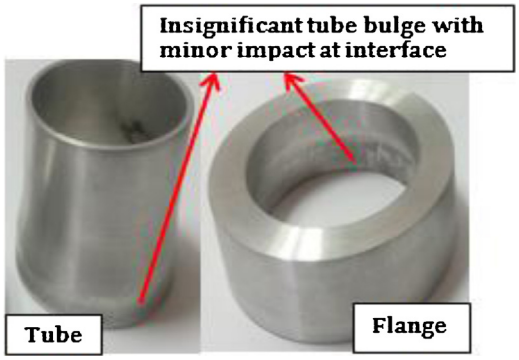

Fig. 14. 50 mm diameter, 1.5 mm thick tube with 2 mm stand-off distance.

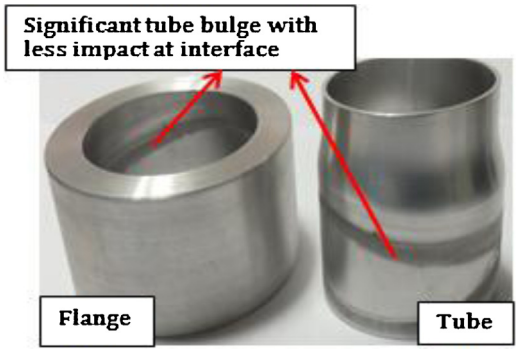

Fig. 15. 50 mm diameter, 1.5 mm thick tube with 3 mm stand-off distance with 3 mm stand-off distance.

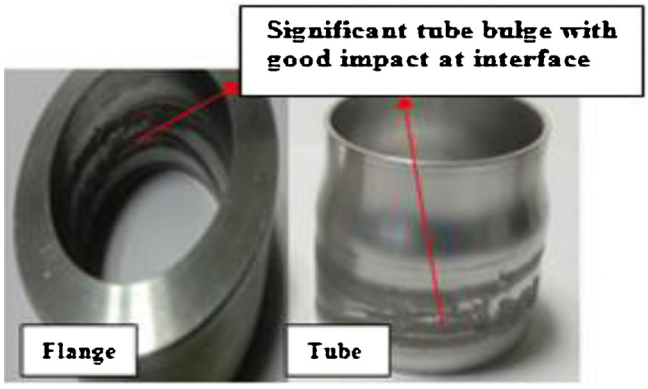

Fig. 16. 50 mm diameter, 1.5 mm thick tube with 2.5 mm stand-off distance.

along with the tube-flange pair was arranged inside a delrin block set-up.

4.1. Effect of system parameters

System parameters like the system frequency and the discharge coil current influences the magnetic pulse expansion welding process. System frequency was seen to play a major role in limiting magnetic field diffusion. Fig. 8 obtained from MATLAB code simulations, shows that with increase in frequency skin depth decreases. This in turn reduces magnetic field diffusion due to which magnetic pressures generated increases, as seen in Fig. 9, thereby increasing the impact velocity.

In the process, the magnetic pressure and the impact velocities reached depends on the discharge damped coil current. The magnetic pressure increases with the increase in coil current, as

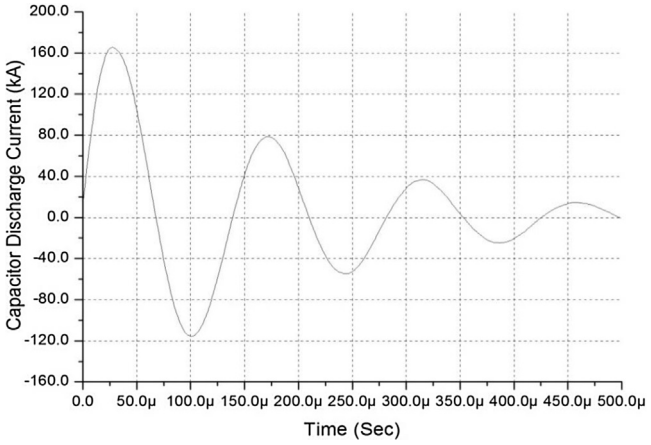

Fig. 17. Capacitor discharge current for expansion welding of 65 mm diameter, 1.5 mm thick tube.

shown in Fig. 10, and this ultimately increases the maximum impact velocity.

4.2. Effect of geometrical parameters

4.2.1. Diameter of tube

It is observed that at 20 kJ energy level, a smaller dimension i.e. 25 mm diameter welded tube-flange pair passed the drop, pull out and peel off tests, as shown in Fig. 11a. Whereas, at the same 20 kJ energy level, a relatively bigger i.e. 50 mm and 65 mm diameter tube-flange pair failed to give similar results, as seen in Fig. 11b. This is because the input energy provided was insufficient to cause significant deformation in the bigger diameter tube and to accelerate it in order to cause a bond at the interface. A bigger size tube has more material and hence requires more energy to be deformed and accelerated than a smaller size tube. Hence, further experiments were performed on 50 mm and 65 mm diameter tube with 40 kJ capacitor bank.

4.3. Thickness of the tube

A thicker tube will have higher impact energy due to higher weight, but it will eventually increase the pressure required to deform as well as to accelerate it towards the other work piece. To study the effect of tube thickness deformation studies were done at 120 kA and it was observed that a 65 mm diameter, 1.5 mm thick tube deforms more in comparison to 2 mm thick tube, as seen in Fig. 12. For the same input energy, a thinner tube accelerates to high impact velocities whereas the maximum impact velocity that can be achieved decreases for a thicker tube. This is because in case of a thinner tube relatively less energy of the total available energy is utilized to deform it and rest of the energy is used in achieving high collision velocities. When stand-off was maintained 2.5 mm, the peak impact velocity reached is lower for a 2 mm thick tube than for 1.5 mm thick tube, as seen in MATLAB simulation plot in Fig. 13. In case of a thicker tube, more energy is utilized in deforming it and with the remaining energy the tube is unable to reach to the required collision velocity.

4.4. Stand-off distance

To study the effect of stand-off distance, simulation studies and EM expansion experiments at an input energy of 150 kA were done on a 50 mm and 65 mm diameter, 1.5 mm thick tube with stand-off distance 2 mm, 2.5 mm and 3 mm. The effect of thickness and stand-off distance on the maximum impact velocity that can be

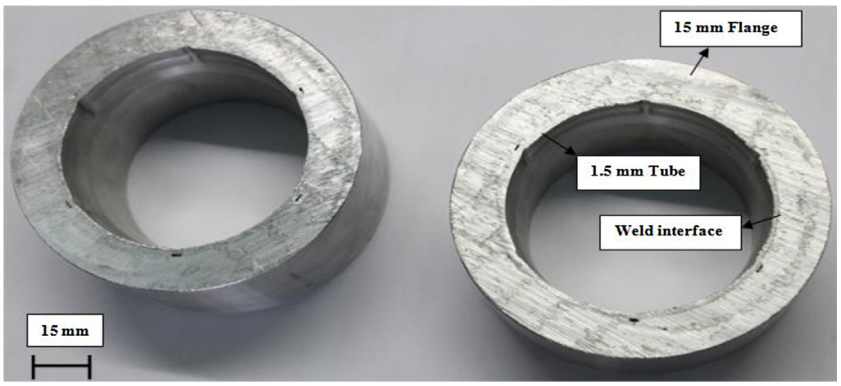

Fig. 18. Laterally cut Al-6061 tube-flange EM expansion welded sample.

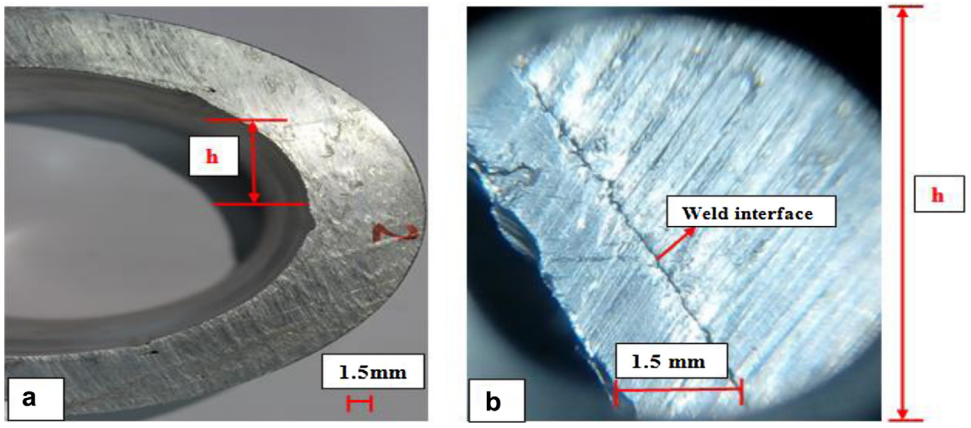

Fig. 19. (a) 10× microscopic image of the tube-flange weld interface, (b) 60× microscopic image showing the tube-flange weld interface.

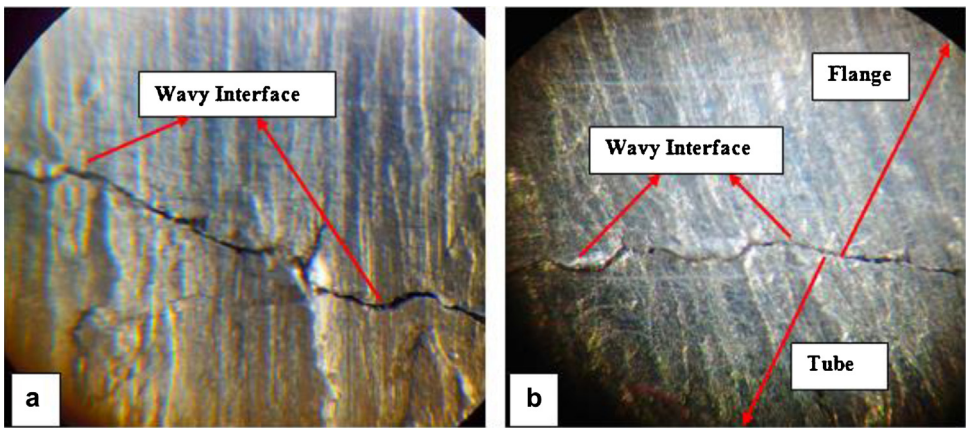

Fig. 20. (a, b) 160× microscopic image showing the wavy interface of the welded tube-flange pair.

achieved at a particular discharge current value is shown in Fig. 13. The peak impact velocity reached is highest for 3 mm stand-off distance followed by 2.5 mm and then 2 mm, as observed from MATLAB simulation plot in Fig. 13 and Table 1.

When stand-off distance was maintained 2 mm there was less impact at the interface, as seen in Fig. 14. This is because 2 mm stand-off distance is inadequate, which causes the impact to occur before the peak pressure and peak impact velocity is reached. The impact velocity for 1.5 mm thick tube with stand-off 3 mm is highest. But from experimental results for 3 mm stand-off distance the impact was observed to be insignificant, evident from the minor surface unevenness formed on the interface as seen in Fig. 15. This is because at 3 mm stand-off the impact occurred after the peak pressure and velocity points have passed. At 150 kA discharge current, the tube deformation and surface unevenness caused due to impact on the tube-flange interface is significant for 2.5 mm stand-off distance, as seen in Fig. 16. This is because at the discharge energy, 2.5 mm stand-off distance was sufficient to cause the impact around the peak impact velocity, V_c and peak pressure, P, as seen in Fig. 3.

For a peak current value of 166 kA, as seen in Fig. 17, it was observed that a good quality weld was achieved for 65 mm diameter, 1.5 mm thick tube to 15 mm thick flange with 2.5 mm stand-off distance. Whereas, at the same peak current value of 166 kA for 2 mm and 3 mm stand-off distance weaker welds were achieved

Table 1
Impact Velocity obtained by simulation for a particular tube thickness and stand-off distance.

Sl No.	Thickness of tube, t (mm)	Stand-off distance, s (mm)	Current I (kA)	Impact velocity, $\mathbf{V_C}$(m/s)
1	1.5	3	150	760.13
2	1.5	2.5	150	693.90
3	1.5	2	150	620.66
4	2	2.5	150	605.33
5	2	2	150	541.42

5. EM expansion welding results of Al 6061

The 65 mm diameter, 1.5 mm tube-flange welded sample passed the pull-out, drop, peel off tests and a distinct weld interface with material interflow was seen, as in Fig. 18 which shows the laterally cut welded tube-flange pair. Weaker weld at 3 mm stand-off distance was observed because for higher stand-off the tube has to deform more requiring more energy for deformation, which ultimately decreases the impact velocity. For lower stand-off distance of 2 mm, weld was weak because the impact occurred before the peak pressure and the highest velocity could be reached. The stand-off distance should be high enough so that the work piece gets sufficient time to accelerate up to the highest velocity and impacts at the peak pressures generated during the process. But at the same time stand-off distance should not be too high to ensure that tube has not started to deaccelerate crossing the peak impact velocity and pressure points. This otherwise would cause the impact to occur at lower pressure and lower velocity, resulting in a weak or no bond. Hence, the optimal stand-off distance for a particular tube thickness can be arrived experimentally because the complex phenomena of deformation and acceleration are not implemented in the formulae involved. The formulae used, based on literature survey can give only an idea of the impact velocity and the various process parameters.

Experimentally it was found that for a 65 mm diameter and 1.5 mm thick tube, 2.5 mm is the optimal stand-off distance, at which the impact velocity of 660 m/s is reached. Since, a good quality weld was achieved at stand-off 2.5 mm for a peak current of 166 kA; it is evident that the impact in this case occurs near about the highest velocity and peak pressure of 360 MPa.

It was observed that the weld interface had a wavy nature, as seen in Figs. 19 and 20. The flow of material also confirms the formation of jet at the interface of the tube and flange due to the high impact velocities. This jet formed of both the surface material during the impact of one work piece on the other work piece was sufficient to clean the surfaces of oxides and contaminants eliminating the need for pre-cleaning.

6. Conclusions

A 40 kJ MPW system has been designed, developed and commissioned for expansion welding of Aluminium alloy tubes. The short circuit discharge frequency of the system is 20 kHz. The research work presented in this paper has highlighted the crucial parameters that have a major influence on the result of expansion MPW of Al 6061 tube to flange. It is seen that the system frequency affects the magnetic field diffusion and the skin depth. The MPW expansion coils fabricated with rectangular cross section copper wires were found mechanically stronger and developed 1.3 times higher fields than the coils fabricated of circular cross section copper wires. The MP expansion welding is influenced by geometrical parameters like diameter, stand-off distance between the work pieces and thickness of tube. For a 65 mm diameter, 1.5 mm thick tube at a discharge current of 166 kA corresponding to 360 MPa peak pressure and 31 T magnetic field, 2.5 mm is the optimal stand-off distance which resulted into a metallurgical bond between the work pieces at the interface. A good quality of weld is obtained when the tube velocity is >600 m/s for a 65 mm diameter, 1.5 mm thick tube and when the impact occurs around the peak pressure and highest velocity. It was also observed that for a particular discharge coil current value, thinner tubes utilized less energy to deform significantly as well as got accelerated to higher velocity in comparison to relatively thicker tubes. Moreover, on analysing the weld joint wavy nature of the weld interface was observed and flow of material confirmed the phenomena of jet formation at the surfaces of the work pieces.

Acknowledgements

We sincerely express our deep gratitude to Shri. D. Venkateswaralu, Regional Director, BARC, Visakhapatnam for his support throughout the work. We are thankful to Shri. R.K. Rajawat, Associate Director, Beam Technology and Development Group, BARC, Mumbai for his guidance during the work. We also express our humble and heartfelt gratitude to Dr. Archana Sharma, Outstanding Scientist, Accelerator and Pulsed Power Division, BARC, Mumbai, whose immense knowledge had always been a source of inspiration and motivation to us.

References

Al Hassani, S.T.S., Duncan, J.L., Johnson, W., 1967. The influence of electrical and geometrical parameters in magnetic forming. In: Proceedings of the 8th International MTDR Conference, Manchester, UK, pp. 1333–1348.
Broeckhove, Jan, Willemsens, Len, 2009–2010. Experimental research on magnetic pulse welding of dissimilar metals. Master Thesis, Ghent University, 1–189.
Desai, S.V., Kumar, Satendra, Satyamurthy, P., Chakravartty, J.K., Chakravarthy, D.P., 2010a. Scaling relationships for input energy in electromagnetic welding of similar and dissimilar metals. J. Electromagn. Anal.Appl. 2, 563–570.
Desai, S.V., Kumar, S., Satyamurthy, P., Chakravartty, J.K., Chakravarthy, D.P., 2010b. Analysis of the effect of collision velocity in electromagnetic welding process of aluminium strips. Int. J. Electromagn. Mech. 34, 131–139.
Jassim, Ahmad K., 2011. Magnetic pulse welding technology. Iraq J. Electr. Eng. 7, 169–179.
Kore, S.D., Vinod, P.N., Kumar, S., Kulkarni, M.R., 2012. Study of wavy interface in electromagnetic welds. Key Eng. Mater. 504–506, 729–734.
Koreaki, Tamaki, Matatoshi, Kojima, 1988. Factors affecting the result of electromagnetic welding of aluminium tube. Trans. Japan Weld. Soc. 19, 53–59.
Lee, Sung Ho, Lee, Dong Nyung, 1996. Estimation of the magnetic pressure in the tube expansion by electromagnetic forming. Mater. Process. Technol. 57, 311–315.
Loncke, K., 2009. An Exploratory Study into the Feasibility of Magnetic Pulse Welding. Master Thesis. Ghent University, pp. 1–147.
Miranda, R.M., Tomás, B., Santos, T.G., Fernandes, N., 2014. Magnetic pulse welding on the cutting edge of industrial applications. Soldag. Insp. São Paulo 19, 069–081.
Patel, C., Date, P.P., Kulkarni, S.V., Kumar Satender, Rani Dolly, Kulkarni, M.R., Desai, S.V., Rajawat, R.K., Nagesh, K.V., Chakravarty, D.P., 2009. Electromagnetic welding of AL-to-Al-Li sheets. ASME J. Manuf. Sci. Eng. 131, 1–4.
Rajawat, R.K., Desai, S.V., Kulkarni, M.R., Rani Dolly, Nagesh, K.V., SethiR, C., 2004. Electromagnetic forming-a technique with potential applications In accelerators. In: Proceedings of APAC, Gyeonju, Korea, pp. 187–189.
Umer, Sabith, 2013. Magnetic pulse welding, forming & crimping. mechanical engineering. Int. J. Sci. Technol. Res. 2, 79–82.
Vinitha, G., Gupta Pragati, Kulkarni, M.R., Saroj, P.C., Mittal, R.K., 2014. Estimation of charging voltage for electromagnetic welding. Internal Conference on Magnetics, Machines & Drivers (AICERA-2014 iCMMD), 1–4.
Zhidan, X.U., Junjia, C., Haiping, Y.U., Chunfeng, L.I., 2013. Research on the impact velocity of magnetic impulse welding of pipe fitting. Mater. Des. 49, 736–745.